Tuijin Jishu/Journal of Propulsion Technology
ISSN: 1001-4055
Vol. 45 No. 2 (2024)

Mass Irregularities in Conventional Slab Systems and Bubble Deck Slab Systems Comparison

Mr. Sita Ram Prasad[1], Prof. K.L. Radhika[2]

[1]*Postgraduate Student, University College of Engineering, Osmania University.*

[2]*Professor, University College of Engineering, Osmania University*

Abstract: This study provides a thorough comparison of mass irregularities in conventional slab systems as well as bubble deck slab systems. The research includes eight unique models, which range from conventional slabs to flat slabs with and without drops, in both regular and irregular arrangements. To guarantee a thorough analysis, many structural characteristics such as building height, grid spacing, column and beam diameters, floor-to-floor height, and material qualities have been thoroughly determined. The goal of this research is to compare & contrast the performance of these slab systems in terms of key structural performance indicators such as max. storey displacement, storey drift, base shear, joint displacements, axial forces, bending moments, shear forces, time periods, and modal frequencies. The findings of each model are investigated using thorough finite element analysis performed using ETABS software under both non-irregular and mass irregular circumstances. These results are intended to give useful insights into how conventional and bubble deck slab systems react to dynamic pressures, allowing for a better understanding of their performance and resilience in actual engineering applications. The study's goal is to help structural engineers and architects make educated selections when deciding between these two high-rise slab systems.

***Keywords*:** Conventional Slab, Bubble deck slab, Irregularity, ETABS, RCC building etc.

Introduction:

In contrast to other construction materials, reinforced concrete (RC) is both cost-effective and structurally sound. Consequently, it has emerged as the most frequently employed construction material. However, one drawback of concrete is its excessive density in relation to its strength, resulting in RC buildings being considerably heavier in weight compared to steel structures, [1], [2]. As they comprise a significant portion of the building's mass, to reduce the weight of the RC structures, the weight of the slabs must be decreased. Moreover, sustaining structural elements such as columns, beams, and foundations are unnecessary for slabs with a reduced heft. A decrease in the total mass of a structure consequently results in enhanced performance under seismic forces. In the past, considerable effort has been devoted to substantially reducing the surface bulk. In 1990, one of the proposals put forth by Danish engineer Jrgen Breuning was the implementation of bubble slabs.[3]. Due to the introduction of a series of cavities within slabs with inefficient concrete, a considerable amount of concrete detaches in this form of slab. Void introduction can result in a reduction of slab weight by 35-50%. [4]–[7] Multiple varieties of voids, which are frequently made of lightweight materials such as polystyrene or plastic, were utilized. [7].

As it provides space, the foundation is an essential structural component in construction projects. Furthermore, among the components, the surface utilizes the most concrete. Jorgen Bruenig developed

the first biaxial hollow slab (presently referred to as Bubble Deck) in Denmark prior to inventing Bubble Deck in the 1990s. Recent years have seen the implementation of this innovative prefabricated construction method utilising Bubble Deck slabs in a variety of industrial projects around the world. Using porous spheres made from recycled plastic, Bubble Deck slab is an innovative method of practically eliminating the concrete component in the centre of a conventional slab without sacrificing structural performance. Consequently, there is a substantial reduction in the structural self-weight, leading to a slab that is 30 to 50% lighter. This weight reduction in turn alleviates the strains on the columns, walls, foundations, and the entire edifice. Bubble Deck is a more sustainable building alternative than conventional concrete floor systems because it decreases concrete usage. Additionally, it accomplishes sustainability goals through the utilisation of recycled plastic spheres and discharges less CO2 into the environment during the production process. Whether the structure is subsequently demolished or reconstructed, the spheres could potentially be recycled. To increase energy efficiency, the empty air cavity in the hollow spheres may be filled with polystyrene, which provides insulation. In contrast to conventional concrete slabs, the Bubble Deck provides a multitude of advantages, such as a reduced material consumption, enhanced structural efficiency, expedited construction period, and environmentally sustainable status. Two meshes comprise the reinforcements, one positioned at the lower end and the other at the upper end; these meshes can be joined via knotting or welding. The distance between the bars remains constant in accordance with the dimensions of the bubbles to be incorporated and the amount of support provided by the slab's transverse and longitudinal ribs. [7]. In recent times, an abundance of research has been devoted to determining the flexural strength of bubble slabs. According to these studies, the flexural capabilities of two-way bubble slabs are comparable to those of conventional slabs. Nevertheless, marginal decreases in rigidity were detected. [8] [9] [10]. According to Corey [11], Similar strength to that of solid slabs can be achieved by integrating cavities beneath the neutral axis of the slab, more precisely in the tension zone. Nevertheless, the flexural rigidity experiences a decline of 10-20% due to the diminished cross-sectional area provided by spherical cavities. Wondwosen [12] The rigidity of void slabs decreased proportionally to that of solid slabs of equivalent thickness. Nimnim and Zain Alabdeen [13] argued that cube-shaped voids in slabs decreased their strength in comparison to spherical voids, whereas Fatma and Chandrakar disagreed. The influence of void configuration on the strength of slabs was investigated. In contrast to their flexural strength, the striking strength of voided slabs was considerably diminished by their proximity to columns; thus, in order to avert premature calamitous shear collapse, voids ought to be positioned at a distance from columns. [4], [14], [15]. One-way slabs facilitate unidirectional force transmission to supports; thus, the introduction of cavities in this direction may potentially disrupt the load transmission channel, leading to an immediate collapse. As a result, increased caution should be exercised when depleted slabs are intended for resting in unidirectional scenarios. However, until recent years, research on these surfaces was limited.

Arati Shetkar & Nagesh Hanche [16] An experimental investigation was undertaken on a bubble deck slab system that employed elliptical spheres. The performance of the bubble deck slabs was assessed using the ratio of bubble diameter to thickness. Based on the findings, the implementation of bubble deck in construction is considered viable and efficient. At the top and bottom, the reinforcements are arranged as two meshes that are amenable to welding or binding, respectively. As per the specifications of the bubbles to be integrated as Well as the quantity of reinforcement provided by the longitudinal & transverse supports of the slab, the distance between the bars remains constant. The spheres exhibit a diameter variation of 450mm to 180mm. There is a range of 230mm to 600mm in slab depth. The minimum distance between bubbles that is permissible is 1/9th of the diameter of each bubble. The

nominal diameters of the intervals could be 315mm, 180mm, 225mm, 270mm, or 360mm. In shape, bubbles can be either spherical or elliptical. In this experiment, force is applied in the opposite direction of gravity from the bottom to the top of the surface using a hydraulic lift. When this force is applied, it becomes more straightforward to document the deformation and strain of the rebar and concrete from the upper side of the platform. Until fissures are identified in the slabs as well as failure mechanisms become apparent. This indicates that by incorporating hollow elliptical spheres, the load-bearing capacity of the Bubble Deck could potentially be enhanced.

Numerous studies on conventional slabs, flat slabs and bubble deck slabs have been conducted for an extended period of time in an effort to better comprehend building pressures. T. Lai [17] Bubble Deck office slabs' structural behaviour was investigated, and their application as lightweight bridge decks was suggested. Corey Midkiff J [18] compared the construction of a two-way reinforced concrete slab with plastic apertures to that of a conventional flat plate reinforced concrete slab. Neeraj Tiwari and Sana Zafar [19] The inquiry centred on the bubble deck slab system, which mitigates the structure's self-weight through the utilisation of plastic hollow bubbles derived from discarded plastic. Immanuel Joseph Chacko et al. [19] The structural behaviour of a Bubble Deck Slab was investigated by modifying variables such as the diameter of the balls. Mahalakshmi S & Nanthini S [20] investigated the bubble deck slab technology for the fabrication of biaxial slabs. Jiji Jolly [21] Bubble deck slabs with elliptical balls exhibited a greater capacity for load bearing than bubble deck slabs with spherical balls, according to experiments conducted on bubble deck slabs featuring spherical and elliptical balls of grades M25 and M30.

Kim et al. [22] A comparative analysis of various void types revealed that the failure mode could be significantly predicted by the geometry of the voids; round box voids performed less accurately in this regard than donut voids. The slabs experienced tensile failure due to the second phase. These results were validated in an additional inquiry. [23]. Sagadevan and Rao [24] examined two void morphologies—cuboid and spherical—and discovered that the structural performance of slabs with these two voids remained unchanged. It was found by Ibrahim et al. that elliptical voids were more favourable than sphere-shaped voids. [25]. Al-Gasham et al. [26] The researchers investigated the correlation between slab depth and void size and discovered that the structural responses of one-way supported slabs with voids smaller than half the slab depth were not substantially modified. Significant degradation in strength as well as other mechanical parameters was noted beyond this threshold, particularly when the ratio exceeded 75 percent. Other research [22], [23] After conducting an examination of the void materials, it was ascertained that the flexural strength of evacuated slabs was enhanced when high-strength void materials such as glass fibre plastic and polypropylene glass fibre were utilised. The instruments for vacuum repair were examined in [22] Furthermore, the results demonstrated a more pronounced enhancement in the behaviour of the material when steel rods were utilised as opposed to spacers to maintain the position of the spheres. Upon comparison of the two methods used to create the voided slabs, it was determined that the filigree method was less effective than the standard procedure. The filigree technique involves the casting of slabs in multiple layers, whereas the fundamental method utilises a single layer to produce the slabs. [27]

Problem Statement:

Design Data:

An examination of the structural behaviour disparities between conventional slab systems as well as bubble deck slab systems constitutes the issue statement pertaining to the comparison of irregularities in mass between these two systems. The research aims to evaluate mass irregularities by comparing the

two systems' performance with regard to storey displacement, storey drift, base shear, & base responses. For the purpose of the inquiry, the bubble deck slab system and the traditional slab system will be simulated using ETABS software. After that, the simulation results will be analysed to ascertain how the mass irregularities of the two systems vary from one another. The research will add to our understanding of the structural characteristics of both traditional as well as bubble deck slab systems. As a result, future construction endeavours may be better informed in their choice of appropriate slab systems. This study contrasts the mass irregularities of conventional slab systems and bubble deck slab systems. An examination was carried out on the G+13-story framework of a conventional edifice featuring a vertical distance of 3.5 metres between each floor. Seismic Analysis of Multi-story RCC Buildings Using the ETABS Software.

Preliminary information necessary for analysis:

Table 1: Considerations for Rectangular Geometry Analysis Parameters:

Parameter	Values
Number of stories	G+13
Base to plinth	4 meter
Grade of concrete	M40
Grade of steel	Fe 500
Floor to Floor height	3.5 meter
Total height of Building	53 meter
Soil Type	Medium
Dead Load	Self-weight of structure
Live load on floors	5 kN/m2
Frame size	30m X 30m building size
Grid spacing	6 m grids in X-direction & Y-direction
Size of column	700mm x 700 millimeter
Size of beam	350mm x 500 millimeter
Depth of slab	250 millimeter
Importance factor for office building	1
Damping percent	5 percent

ETABS Models:

Based on the problem statement outlined in the preceding chapter, the subsequent models are suggested:

MODEL 1	Conventional Slab Building without Irregularity
MODEL 2	Flat Slab Building (with Drop) without Irregularity
MODEL 3	Flat Slab Building (without Drop) without Irregularity.
MODEL 4	Bubble Deck Slab Building without Irregularity.
MODEL 5	Conventional Slab Building with Mass Irregularity

MODEL 6	Flat Slab Building (with Drop) with Mass Irregularity.
MODEL 7	Flat Slab Building (without Drop) with Mass Irregularity.
MODEL 8	Bubble Deck Slab Building with Mass Irregularity.

This document is a summary of models that have been suggested and will be used in a study comparing the stiffness differences between bubble deck slab systems and traditional slab systems. Each model is a distinct version of the slab systems that are being studied.

The research makes use of these models in an effort to assess each slab system's performance in terms of base shear, storey drift, storey displacement, as well as base responses. Finding notable differences in mass abnormalities between bubble deck slab systems and traditional slab systems is the goal of this research.

Modeling:

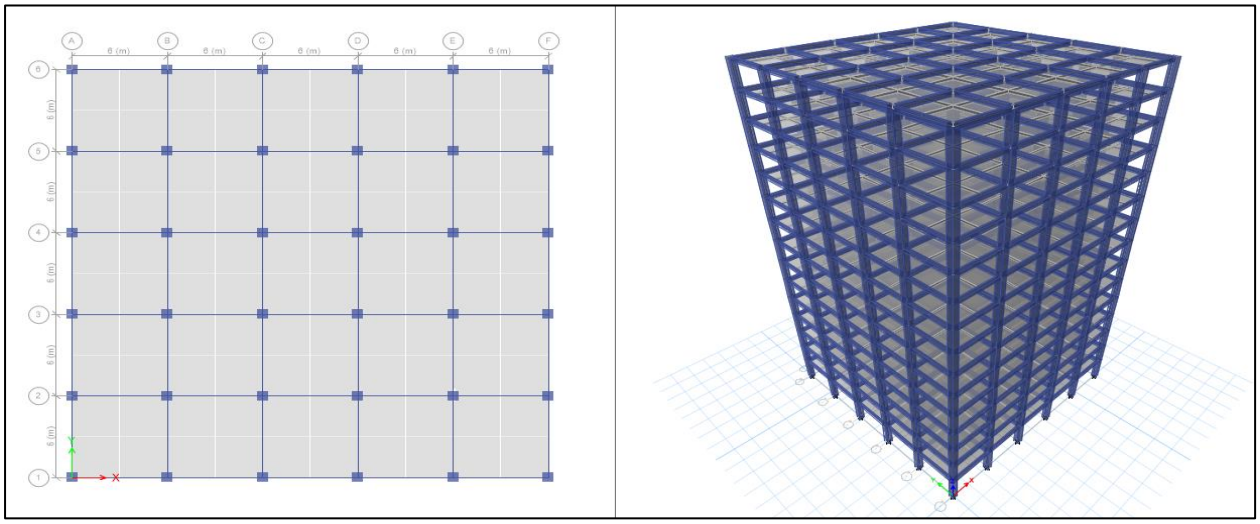

Figure no. 1. Model 1

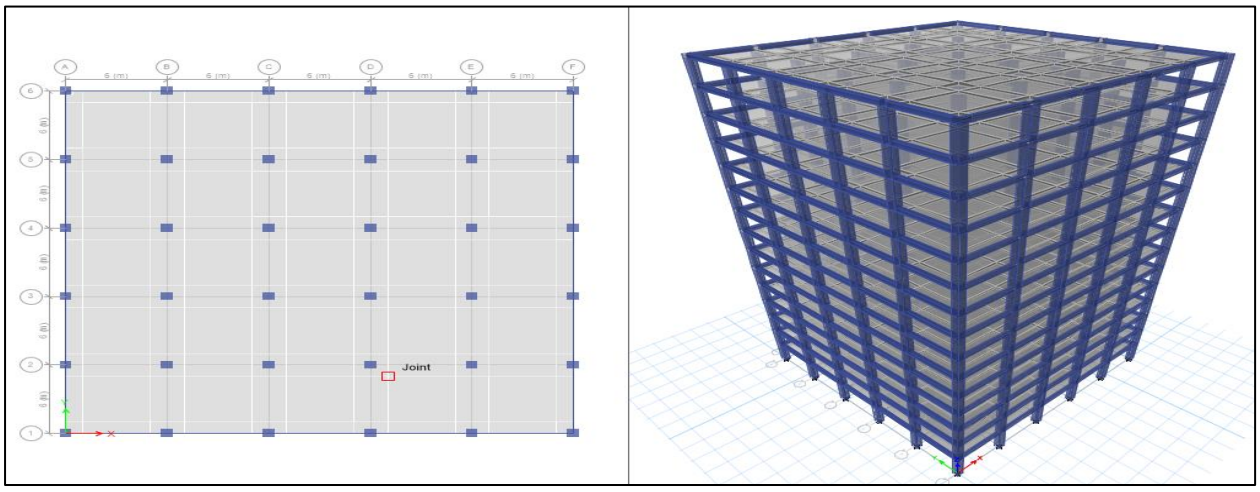

Figure no. 2. Model 2

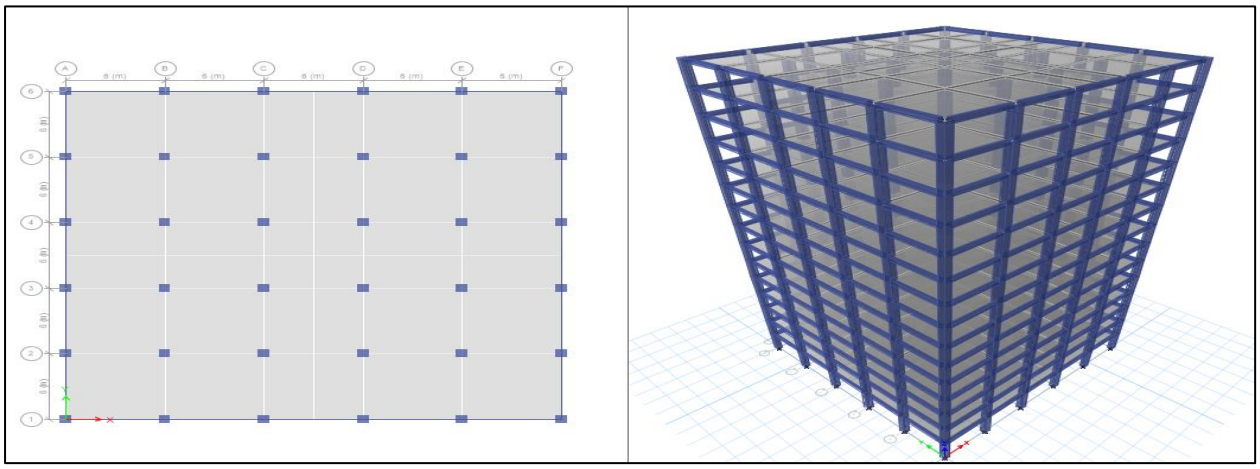

Figure no. 3. Model 3

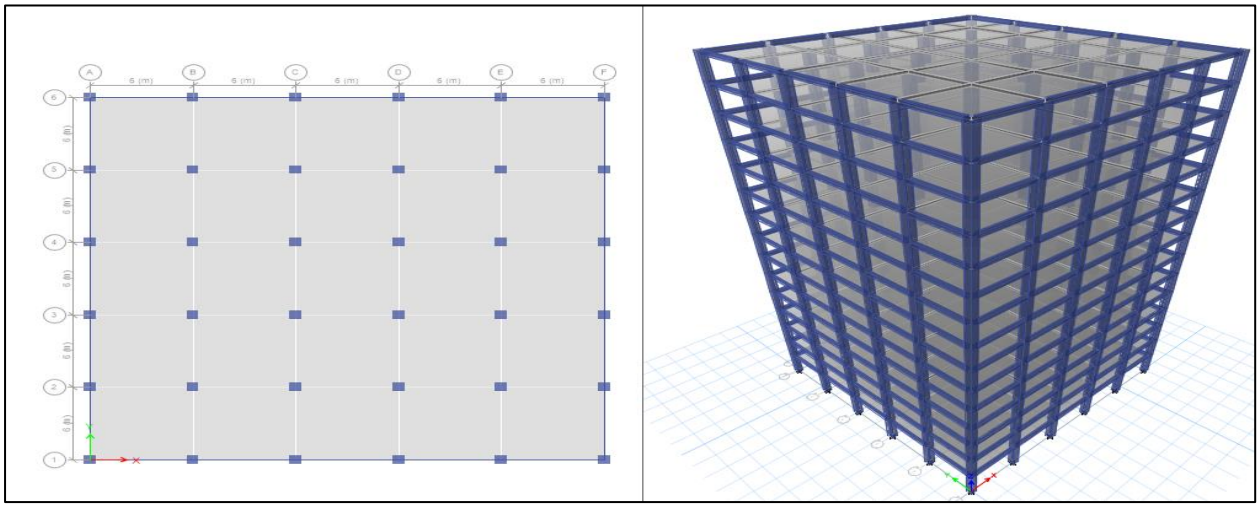

Figure no. 4. Model 4

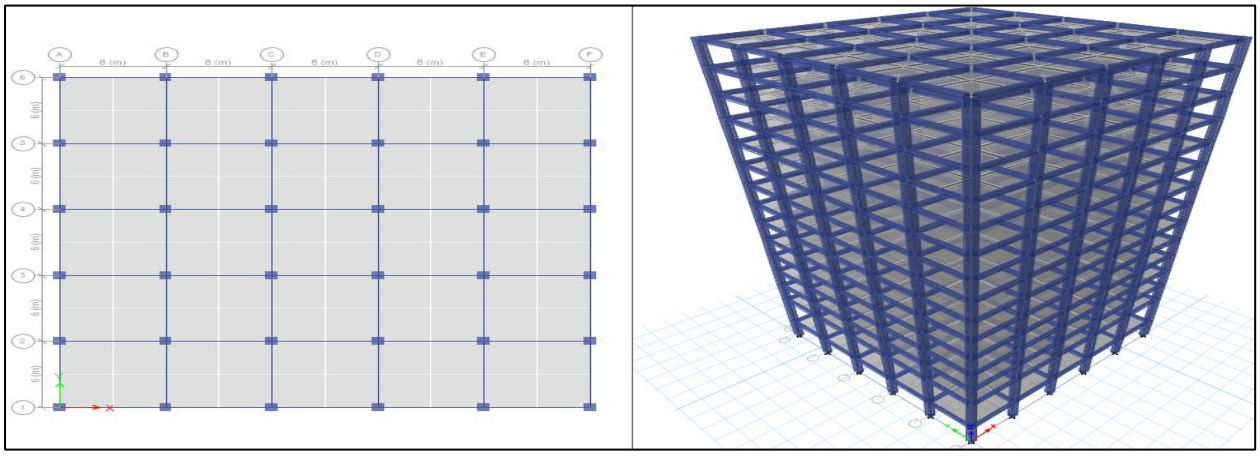

Figure no. 5. Model 5

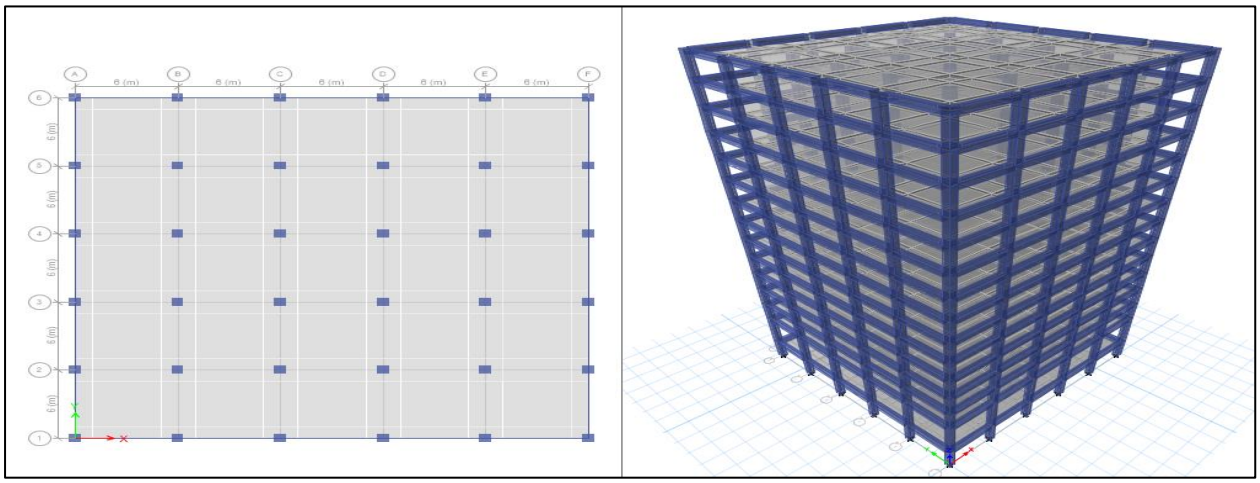

Figure no. 6. Model 6

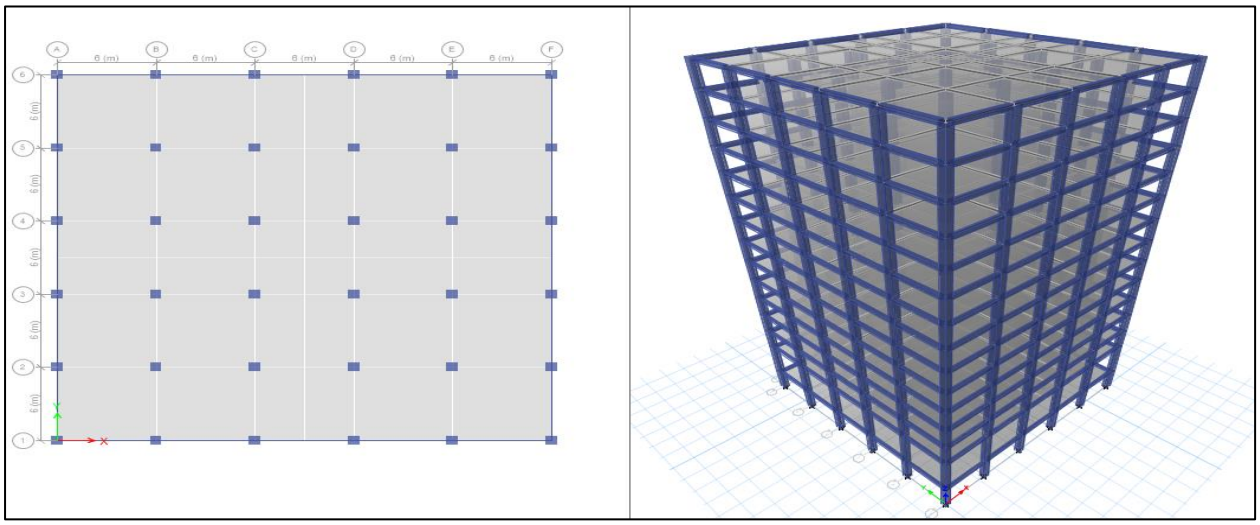

Figure no. 7. Model 7

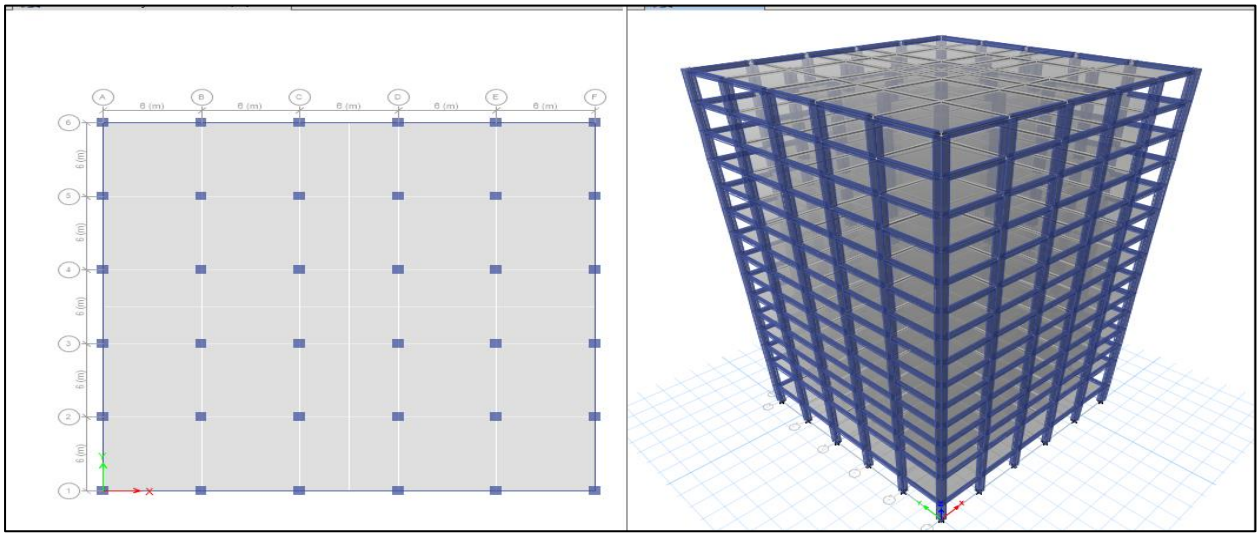

Figure no. 8. Model 8

4. Results And Discussion:

Maximum Storey Displacement in mm

Without Irregularity

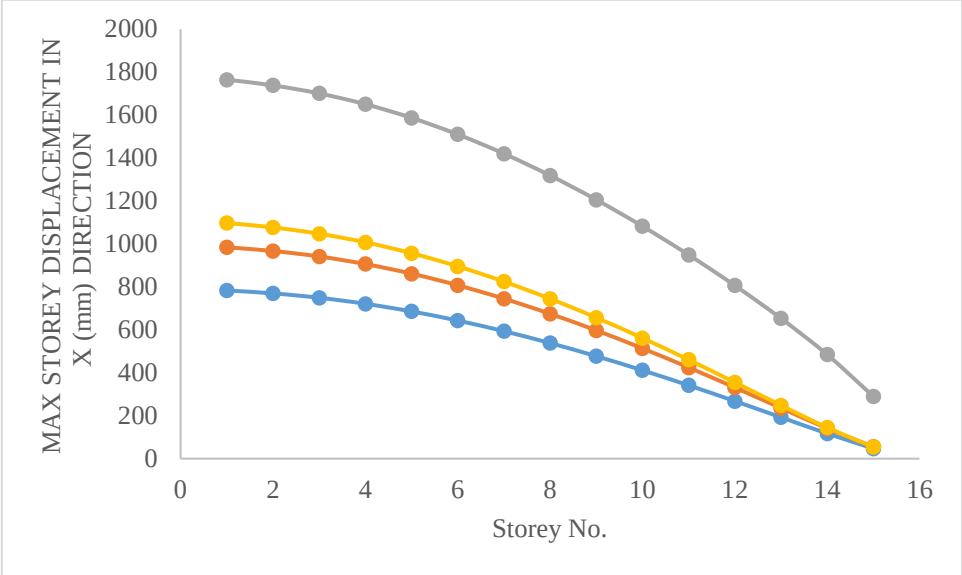

Graph 1: Max Storey Displacement in X (mm) Direction

For each result, the graph above illustrates the Maximum Storey Displacement in millimetres. Maximum Storey Displacement Direction Y Values and Storey No. in the X coordinate. It is apparent that as the storey decreases, the value of Max Storey Displacement diminishes. In the X-direction, the Max Storey Displacement exhibits a maximum value of 1765.094 and a minimum value of 783.451.

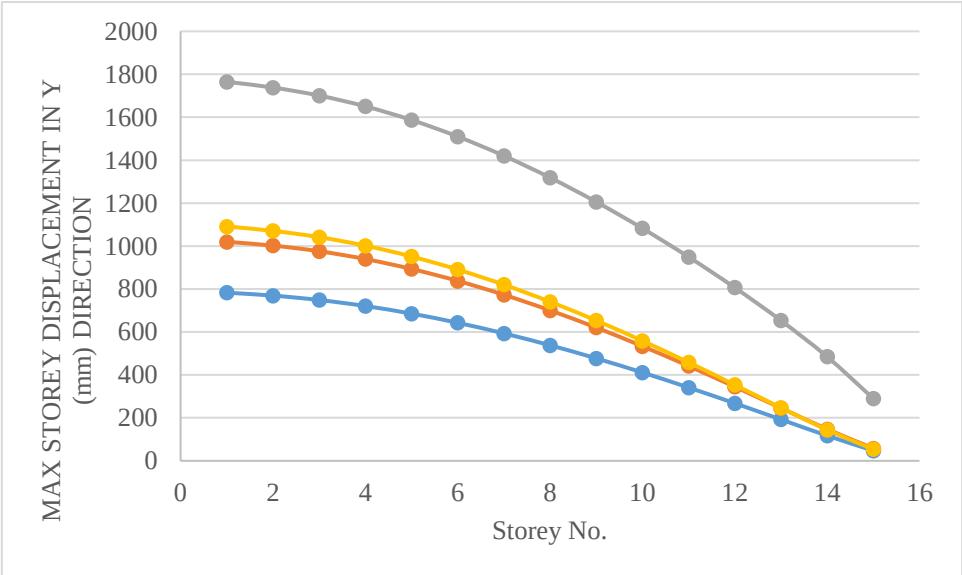

Graph 2: Max Storey Displacement in Y (mm) Direction

The graph above displays the Maximum Storey Displacement in millimetres for each result. Direction Y Values for Maximum Storey Displacement and Storey No. in the X coordinate. It is evident that the

value of Max Storey Displacement decreases as the storey decreases. The utmost value of the Max Storey Displacement in the Y (mm) direction is 1765.094, while the minimum value is 783.009.

With Mass Irregularity

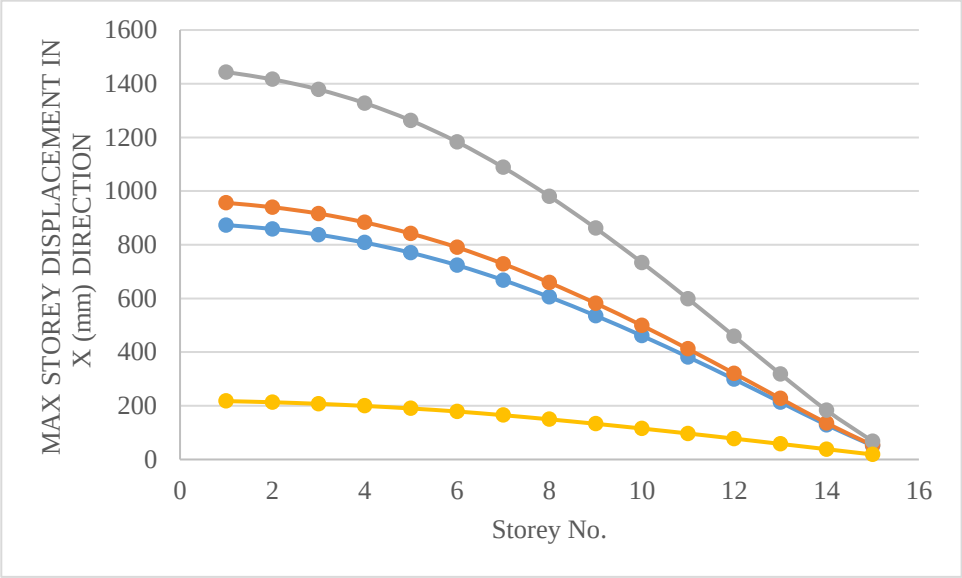

Graph 3: Max Storey Displacement in X (mm) Direction

The graph above displays the Maximum Storey Displacement in millimetres for each result. Direction Y Values for Maximum Storey Displacement and Storey No. in the X coordinate. It is evident that the value of Max Storey Displacement decreases as the storey decreases. The utmost value of the Max Storey Displacement in the X (mm) direction is 1443.275 and the minimum value is 217.384.

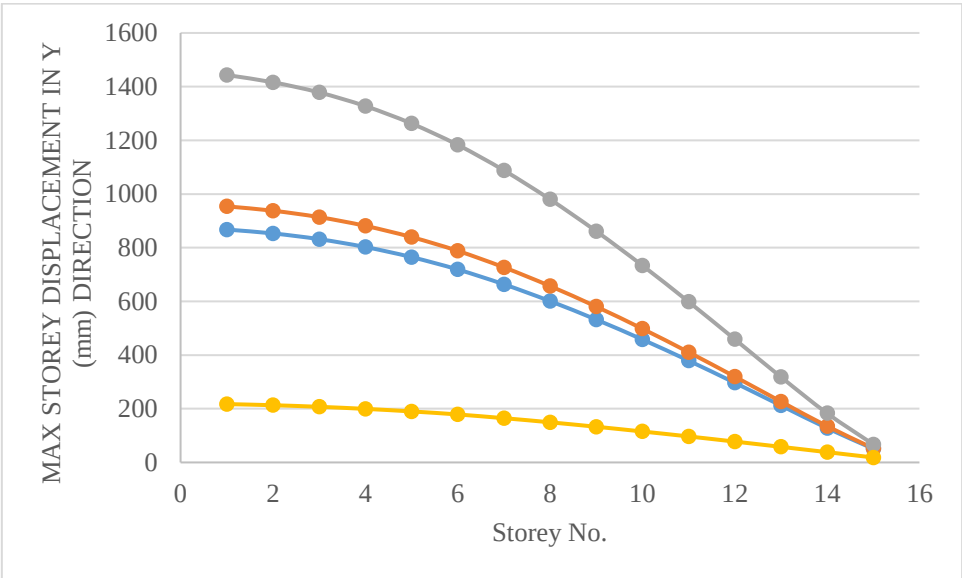

Graph 4: Max Storey Displacement in Y (mm) Direction

The graph above displays the Maximum Storey Displacement in millimetres for each result. Direction Y Values for Maximum Storey Displacement and Storey No. in the X coordinate. It is evident that the value of Max Storey Displacement decreases as the storey decreases. The utmost value of the Max Storey Displacement in the X (mm) direction is 1443.275 and the minimum value is 217.384.

Maximum Storey Drift in mm

Without Irregularity

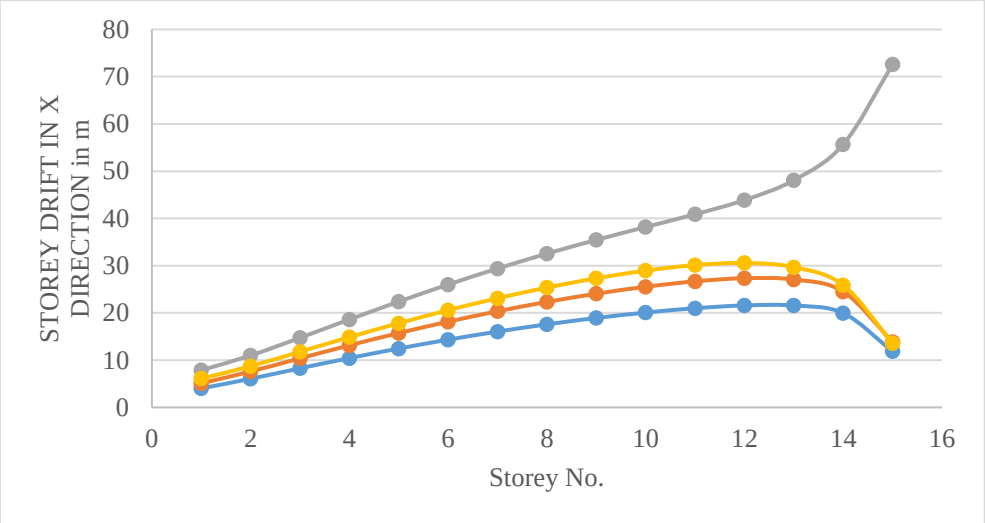

Graph 5: Storey Drift in X direction in (mm) Direction

In millimetres, the aforementioned graph depicts storey drift in the X direction. Wayward Y The X direction indicates maximum storey displacement. Storey No. The X-direction storey drift in millimetres exhibits a maximum value of 7.867 and a minimum value of 4.027.

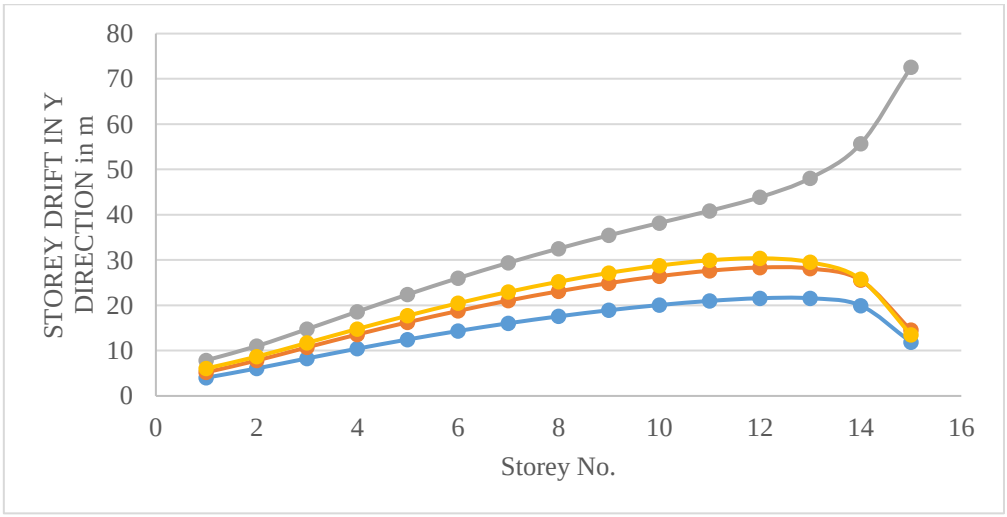

Graph 6: Storey Drift in Y direction in (mm) Direction

The graph above illustrates storey drift in the Y direction measured in millimetres. Direction Y Displays maximum storey drift and X direction No. Storey. The maximum and minimum values for storey drift in the Y direction in millimetres are 7.867 and 4.027, respectively.

With Mass Irregularity

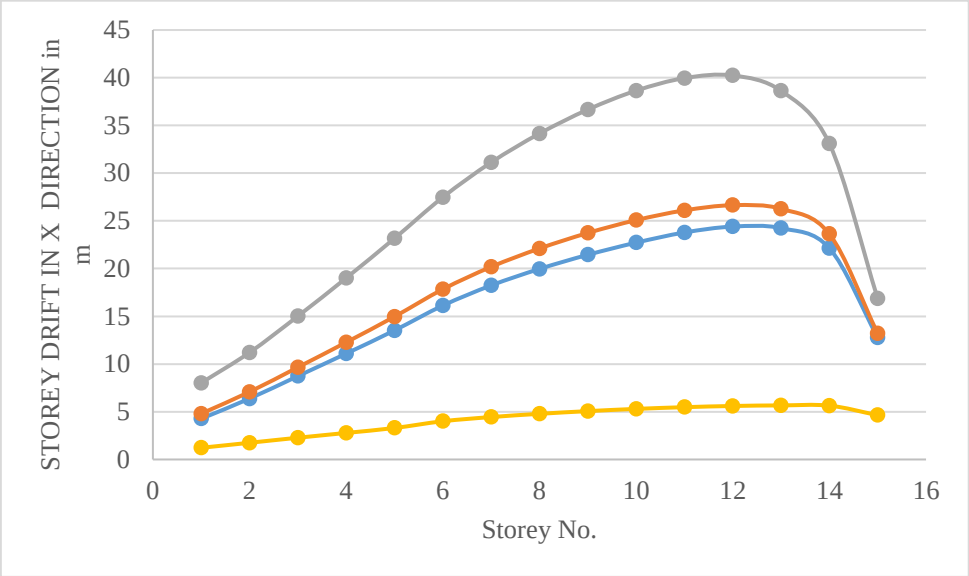

Graph 7: Storey Drift in X direction in (mm) Direction

The graph above displays storey drift in the X direction measured in millimetres. Direction Y Displays maximum storey drift and X direction No. Storey. Maximum storey drift in the X direction is 8.022 millimetres and minimum storey drift is 1.222 millimetres.

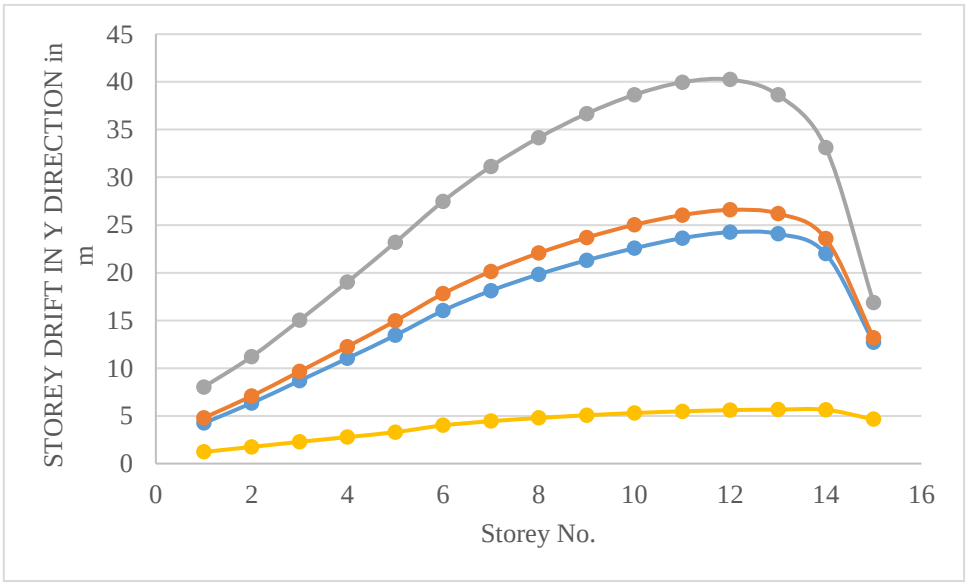

Graph 8: Storey Drift in Y direction in (mm) Direction

The graph above illustrates storey drift in the Y direction measured in millimetres. Direction Y Displays maximum storey drift and X direction No. Storey. Maximum storey drift in the Y direction is 8.022 millimetres and minimum storey drift is 1.222 millimetres.

Storey Stiffness in KN/m

Without Irregularity

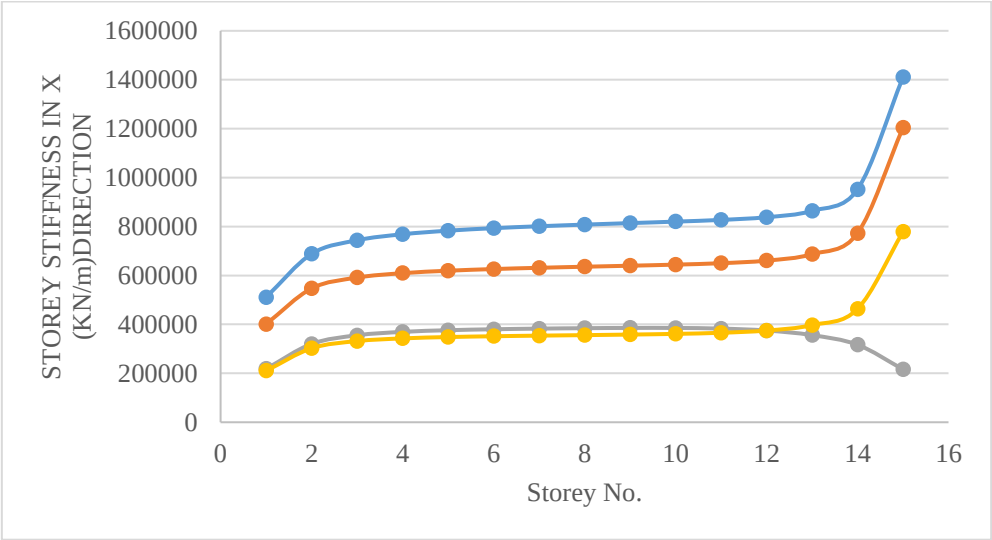

Graph 9: storey stiffness in X(KN/m) direction

The graph above displays storey rigidity values in the X direction, measured in KN/m. Direction Y Indicates storey rigidity, while the X direction indicates storey number. The min. value is 210272.049 as well as the max. value is 510954.683 for storey stiffness in the Y direction in KN/m.

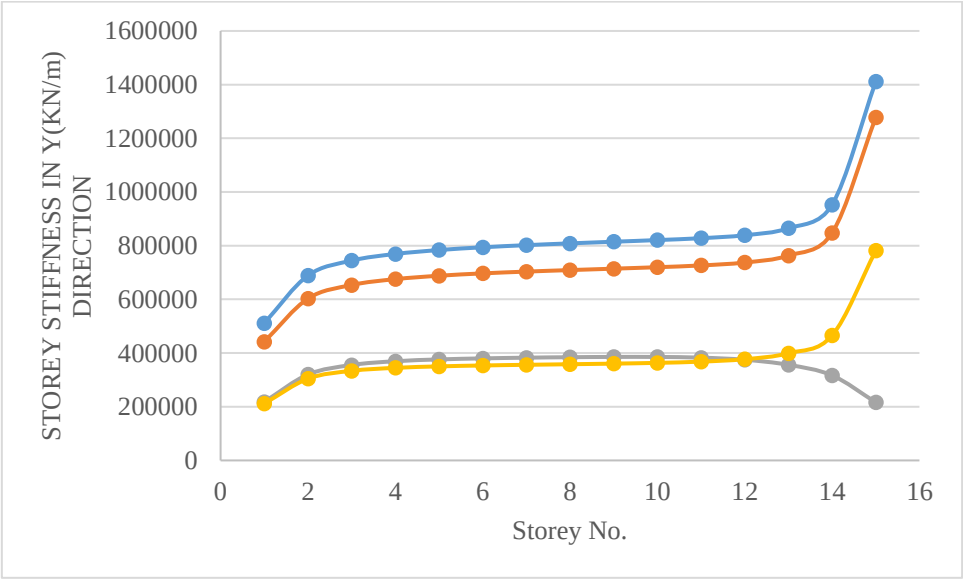

Graph 10: storey stiffness in Y(KN/m) direction

The graph above displays storey rigidity values in the Y direction, measured in KN/m. Direction Y Indicates storey rigidity, while the X direction indicates storey number. For storey rigidity in the Y direction in KN/m, the maximum value is 511366.734 as well as the minimum value is 211733.313.

With Mass Irregularity

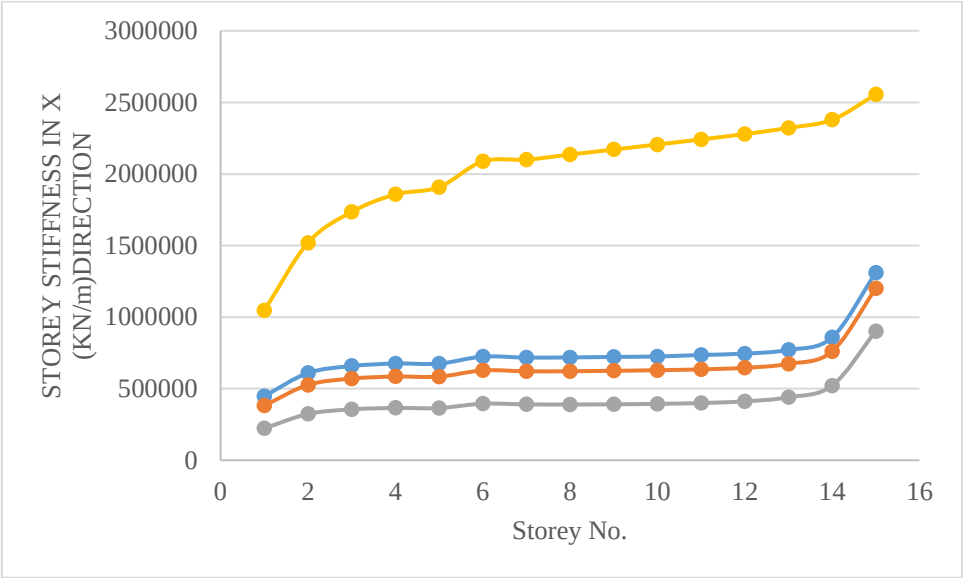

Graph 11: storey stiffness in X (KN/m) direction

The graph above displays storey rigidity values in the X direction, measured in KN/m. Direction Y Indicates storey rigidity, while the X direction indicates storey number. For storey rigidity in the X-direction in KN/m, the maximum value is 1045415.252 as well as the minimum value is 222962.123.

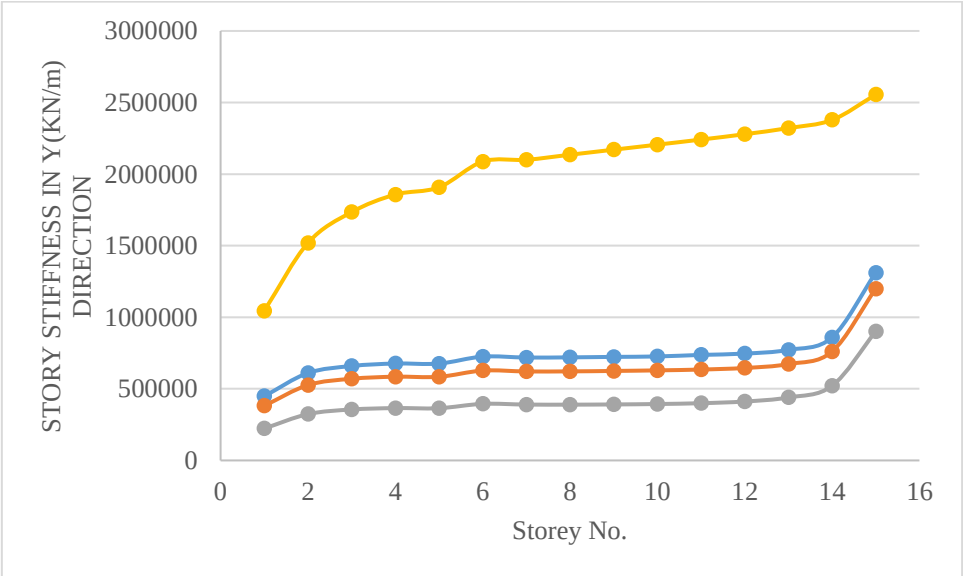

Graph 12: storey stiffness in Y(KN/m) direction

The graph above displays storey rigidity values in the X direction, measured in KN/m. Direction Y Indicates storey rigidity, while the X direction indicates storey number. The minimum value is 210272.049 as well as the maximum value is 510954.683 for storey stiffness in the Y direction in KN/m.

Base Shears in KN

Without Irregularity

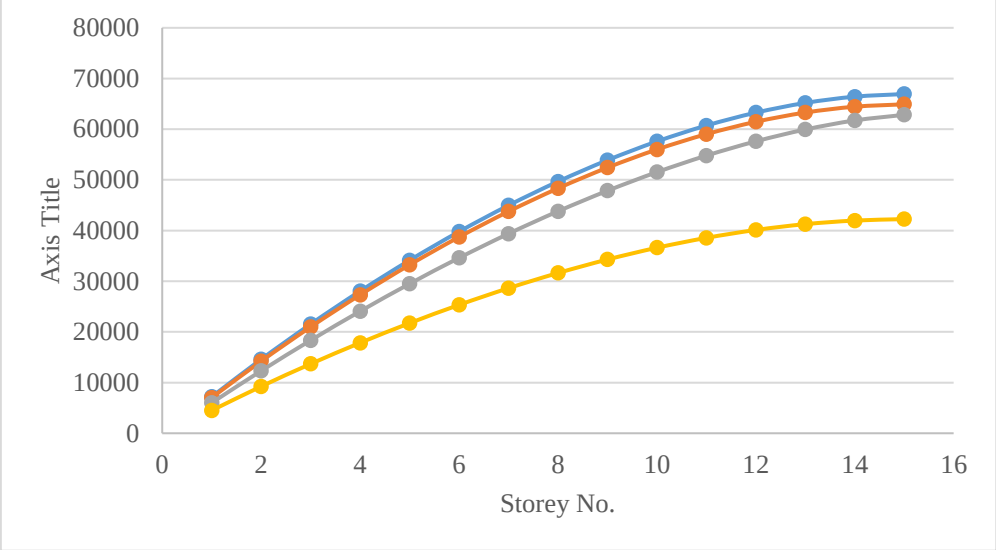

Graph 13: base shear in VX (KN) direction

The graph above displays the results for X-direction base shear in KN. Direction Y Indicated by base shear and storey number in the X direction. The base shear in the X-direction has a minimum value of 4494.5693 as well as a maximum value of 7197.022 KN.

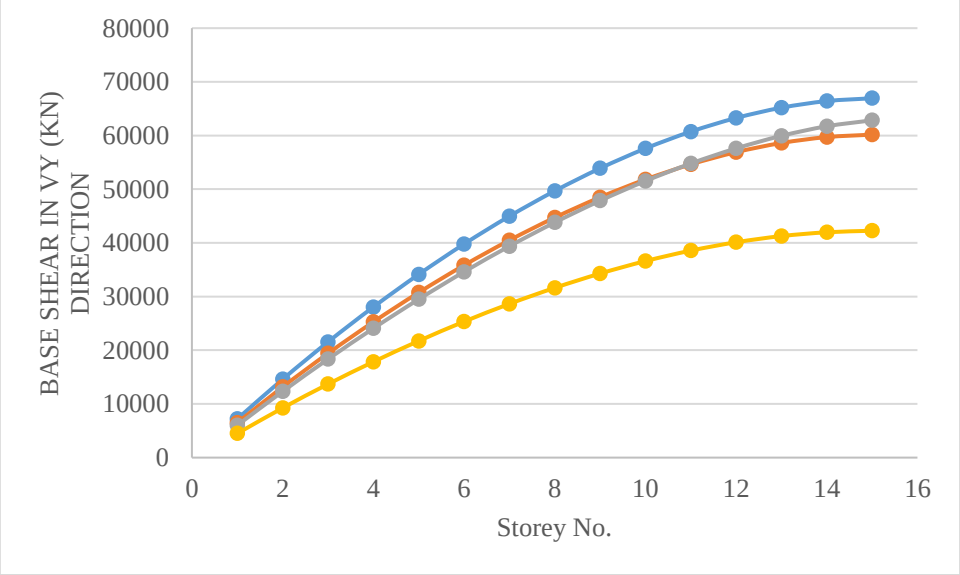

Graph 14: base shear in VY (KN) direction

The graph above displays the results for Y-direction base shear in KN. Direction Y Indicated by base shear and storey number in the X direction. The base shear in the Y direction has a minimum value of 4494.5693 as well as a maximum value of 7197.0218 in KN.

With Mass Irregularity

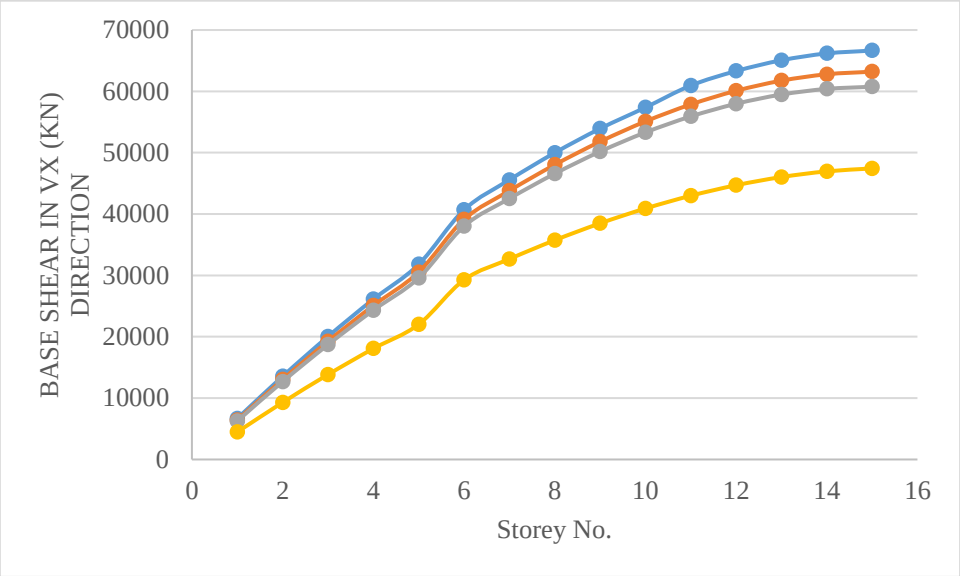

Graph 15: base shear in VX (KN) direction

The graph above displays the results for X-direction base shear in KN. Direction Y Indicated by base shear and storey number in the X direction. The base shear in the X-direction has a minimum value of 4472.0582 as well as a maximum value of 6662.061 KN.

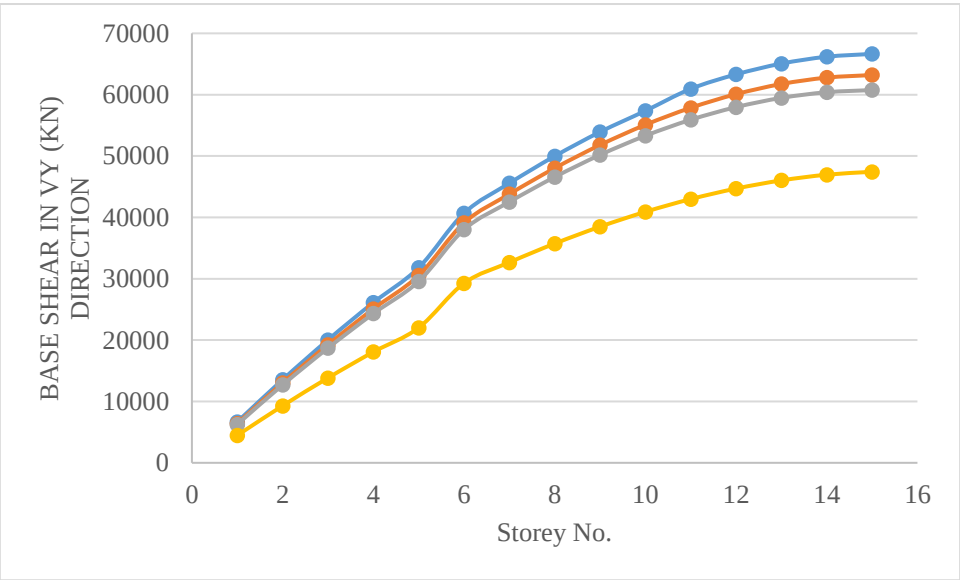

Graph 16: base shear in VY (KN) direction

The graph above displays the results for Y-direction base shear in KN. Direction Y Indicated by base shear and storey number in the X direction. The base shear in the Y direction has a minimum value of 4472.0616 as well as a maximum value of 6662.2178 in KN.

Joint Displacements in mm

Without Irregularity

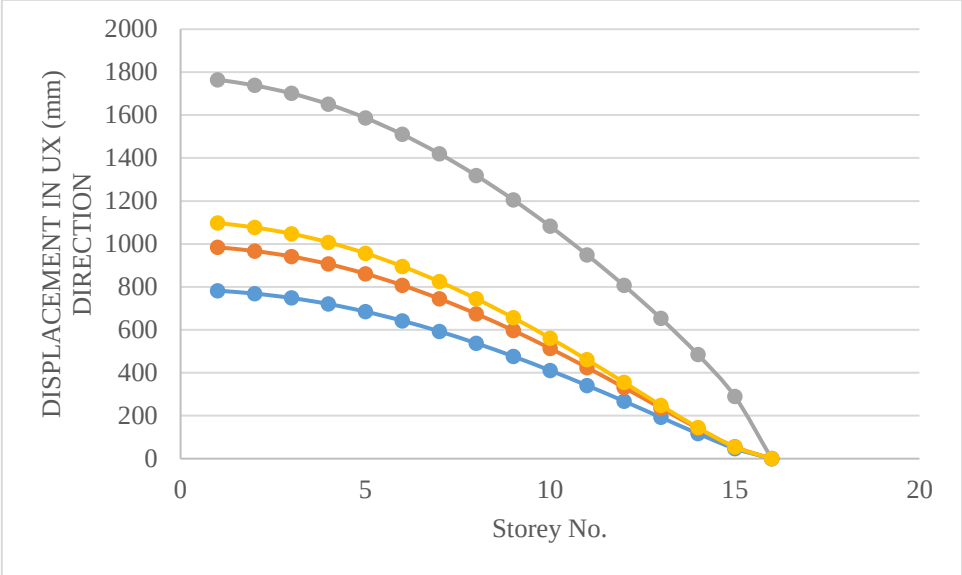

Graph 17: displacement in UX(mm)

The graph above displays displacement values in millimetres along the X-axis. The Y axis represents displacement, while the X axis represents storey number. The upper limit of the displacement in the X direction in millimetres is 1765.094 and the lower limit is 782.448.

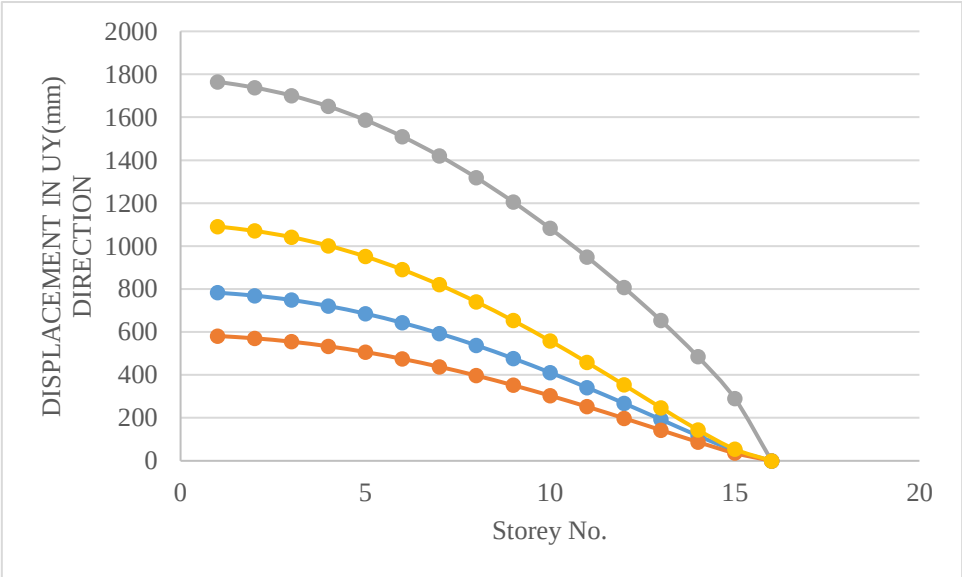

Graph 18: displacement in UY(mm)

The graph above displays the results for Y-direction displacement in millimetres. The Y axis represents displacement, while the X axis represents storey number. Min. value is 581.36 as well as maximum value is 1765.094 for Y-direction displacement in millimetres.

With Mass Irregularity

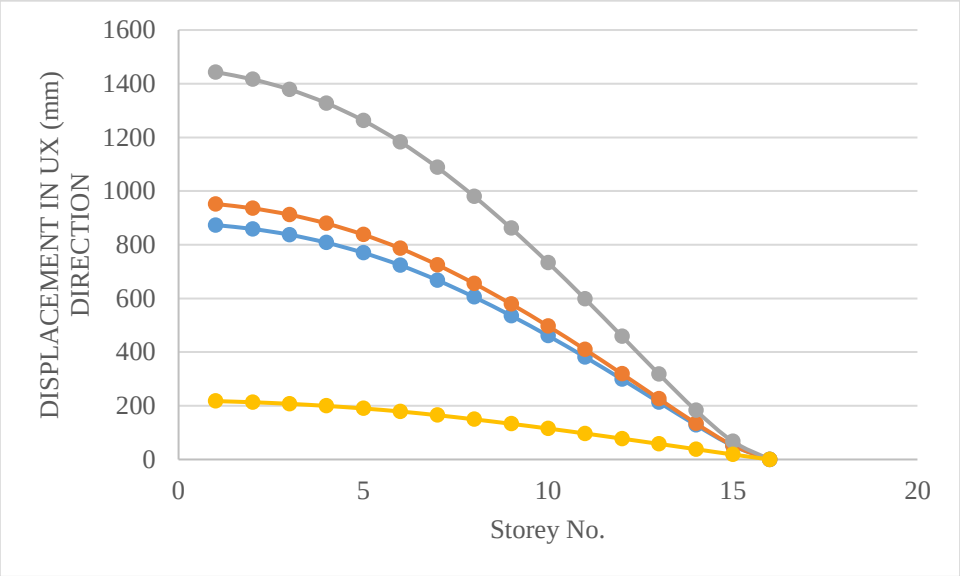

Graph 19: displacement in UX (mm)

The graph above displays displacement values in millimetres along the X-axis. The Y axis represents displacement, while the X axis represents storey number. The X-direction displacement in millimetres contains a maximum of 1443.275 and a minimum of 217.384.

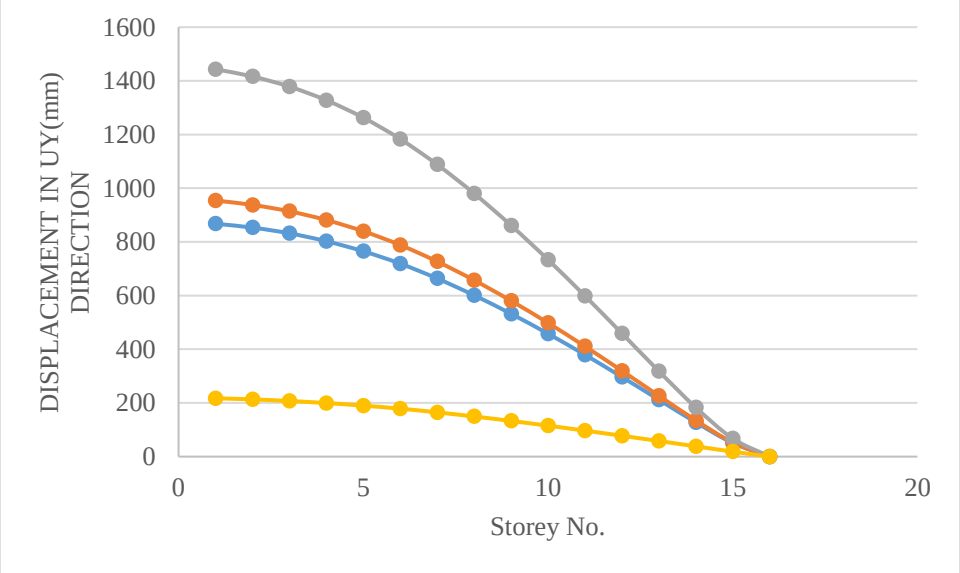

Graph 20: displacement in UY(mm) direction

The graph above displays the results for Y-direction displacement in millimetres. The Y axis represents displacement, while the X axis represents storey number. The Y-direction displacement in millimetres contains a maximum of 1443.275 and a minimum of 217.384.

Axial force in top, middle and bottom most columns in KN-m

Without Irregularity

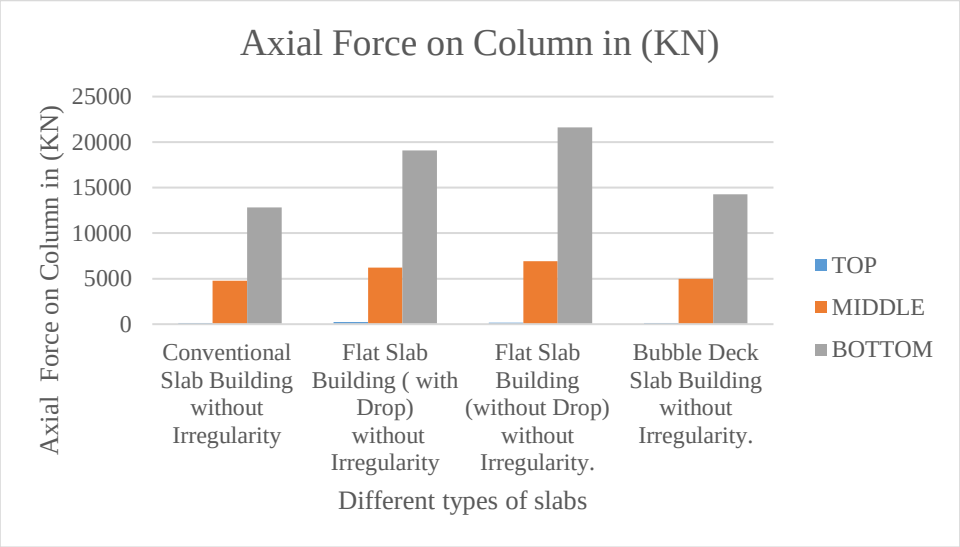

Graph 21: Axial Force on Column (KN)

The graph above illustrates the outcomes pertaining to the Axial Force on Column (KN). The Y-axis represents the Axial Force on Column (KN), while the X-axis represents various slab varieties. The upper, middle, and lower columns each have a maximum value of 242.0987, 6922.8245, and 21604.1646 KN, respectively.

With Mass Irregularity

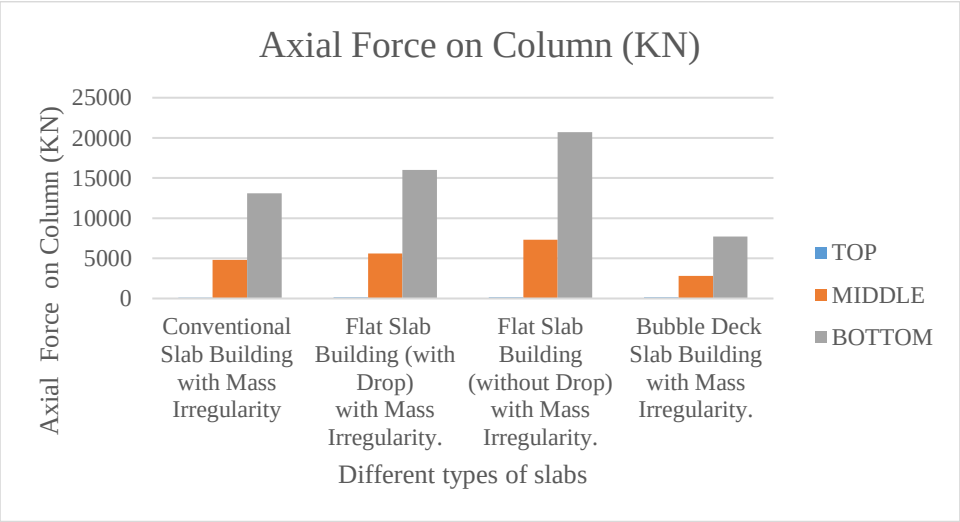

Graph 22: Axial Force on Column (KN)

The graph above illustrates the outcomes pertaining to the Axial Force on Column (KN). The Y-axis represents the Axial Force on Column (KN), while the X-axis represents various slab varieties. In KN, the maximum values for the upper, middle, and bottom columns are, respectively, 141.4923, 7314.5398, and 20722.134.

Bending moment in top, middle and bottom most columns in KN-m

Without Irregularity

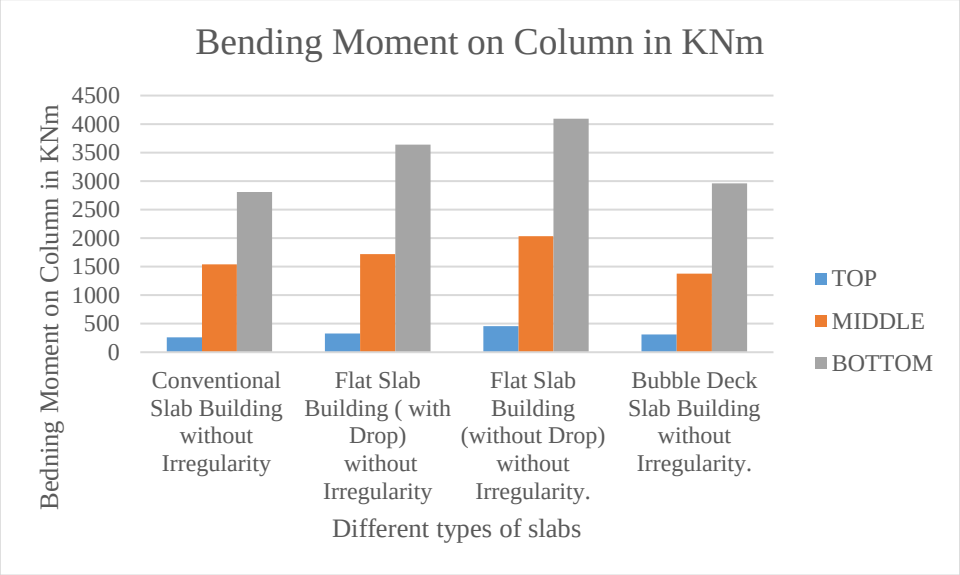

Graph 23: Bending Moment on Column in KNm

The results for Bending Moment on Column in KNm are displayed in the graph above. Y indicates the bending moment on the column in kilonewtons, while X indicates the various varieties of slabs. The upper, middle, and lower columns each have a maximum value of 458.8618, 2033.4605, and 4093.7011 KNm, respectively.

With Mass Irregularity

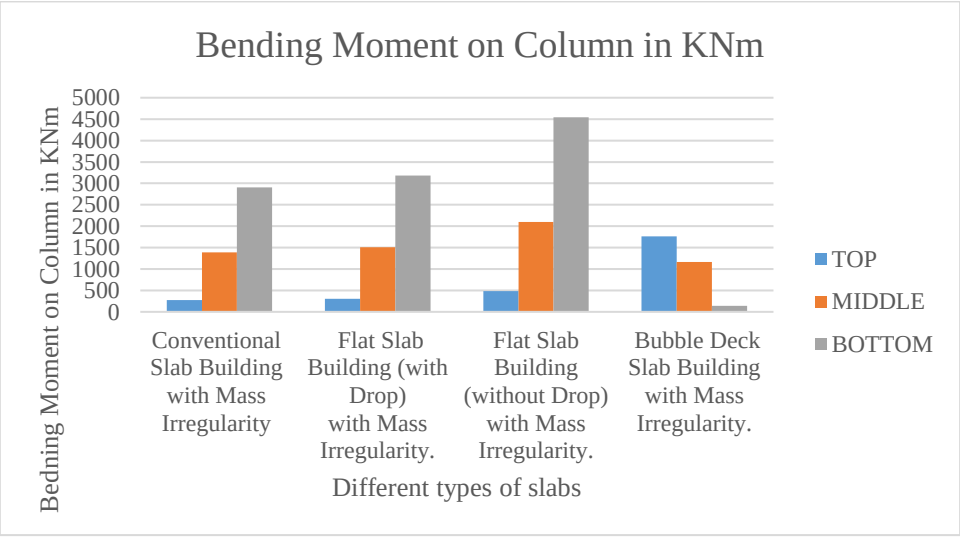

Graph 24: Bending Moment on Column in KNm

The results for Bending Moment on Column in KNm are displayed in the graph above. Y indicates the bending moment on the column in kilonewtons, while X indicates the various varieties of slabs. The upper, middle, and lower columns each have a maximum value of 1762.6541, 2096.1104, and 4546.0638 KNm, respectively.

Shear force in top, middle and bottom most columns direction in KN

Without Irregularity

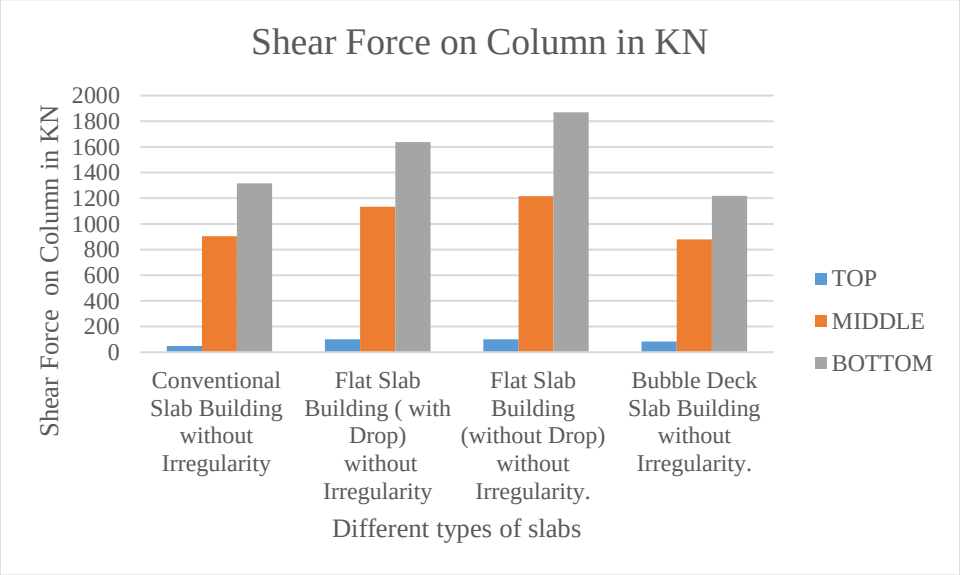

Graph 25: Shear Force on Column in KN

The graph above displays column shear force values in kilonewtons. The Y-axis represents the shear force on the column in KN, while the X-axis illustrates various slab varieties. The maximum values for the upper, middle, and lower columns in KN are 100.872, 1216.1552, and 1869.9302, respectively.

With Mass Irregularity

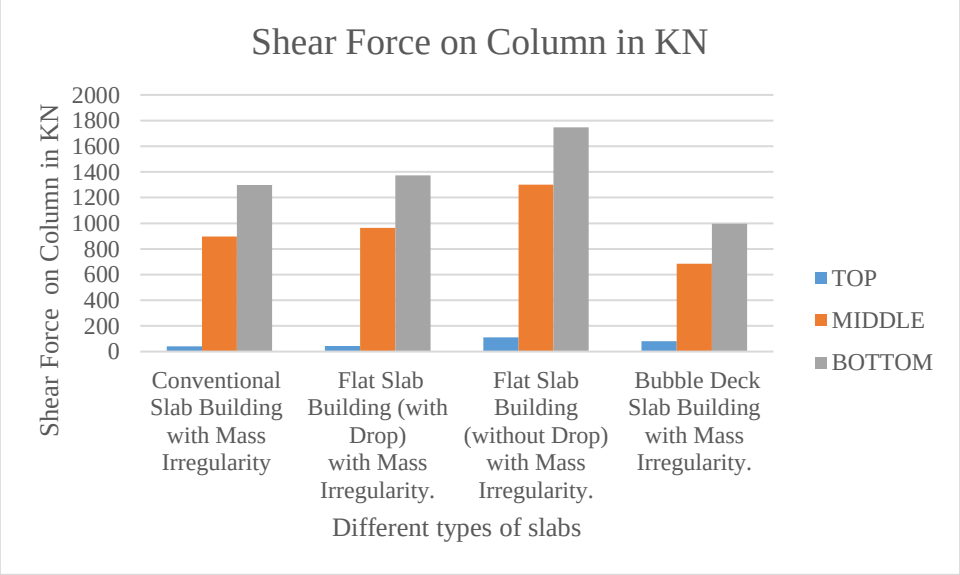

Graph 26: Shear Force on Column in KN

The graph above displays column shear force values in kilonewtons. The Y-axis represents the shear force on the column in KN, while the X-axis illustrates various slab varieties. The highest, middle, and lowest column maximum values in KN are 110.5123, 1299.5519, and 1746.7247, respectively.

Time periods in seconds

Without Irregularity

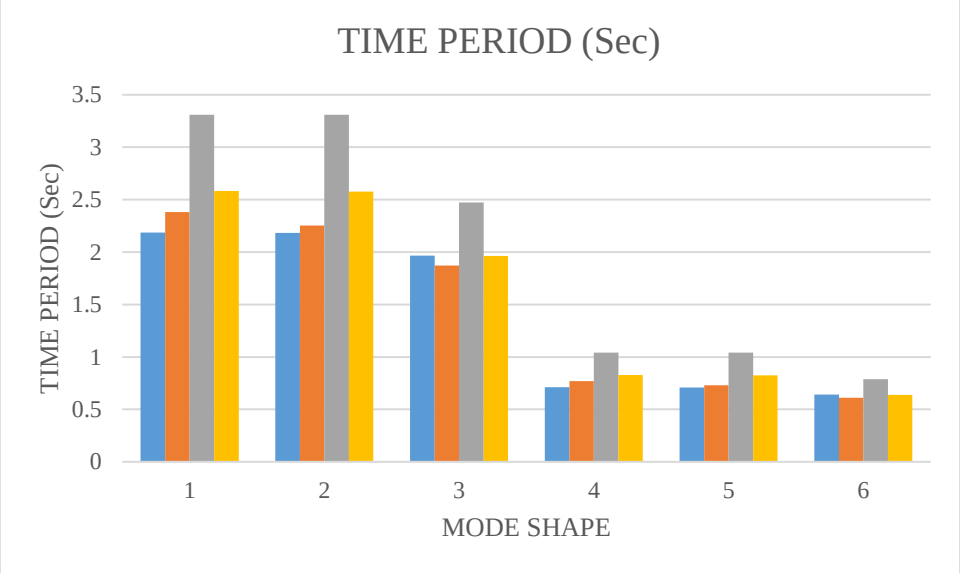

Graph 27: Time Period (Sec)

The graph presented above illustrates the outcomes for the Time Period (Sec). Y represents the time period (seconds), while X represents the mode structures.

With Mass Irregularity

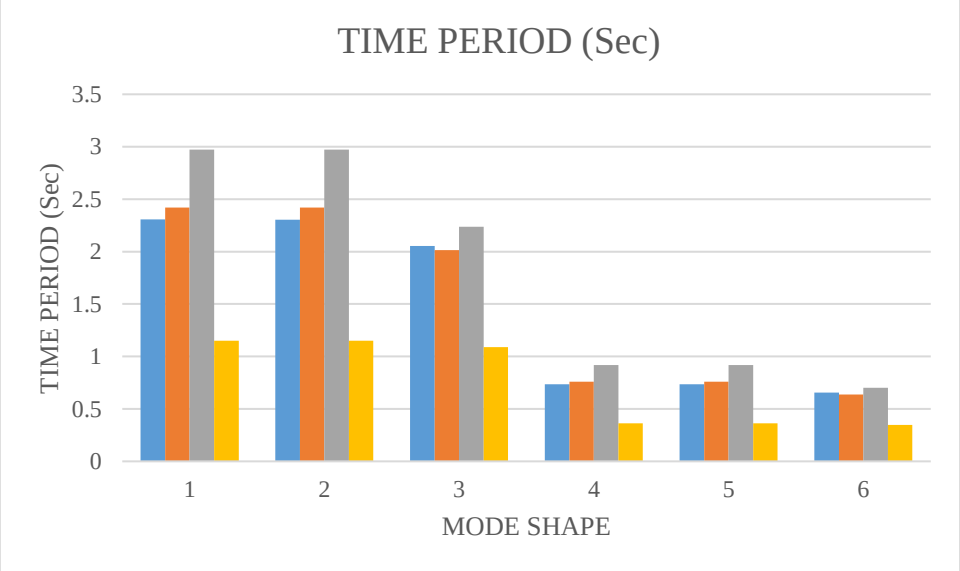

Graph 28: Time Period (Sec)

Results for Time Period (Sec) are displayed in the graph above. X indicates mode shapes, while Y indicates time period (in seconds).

Modal Frequencies

Without Irregularity

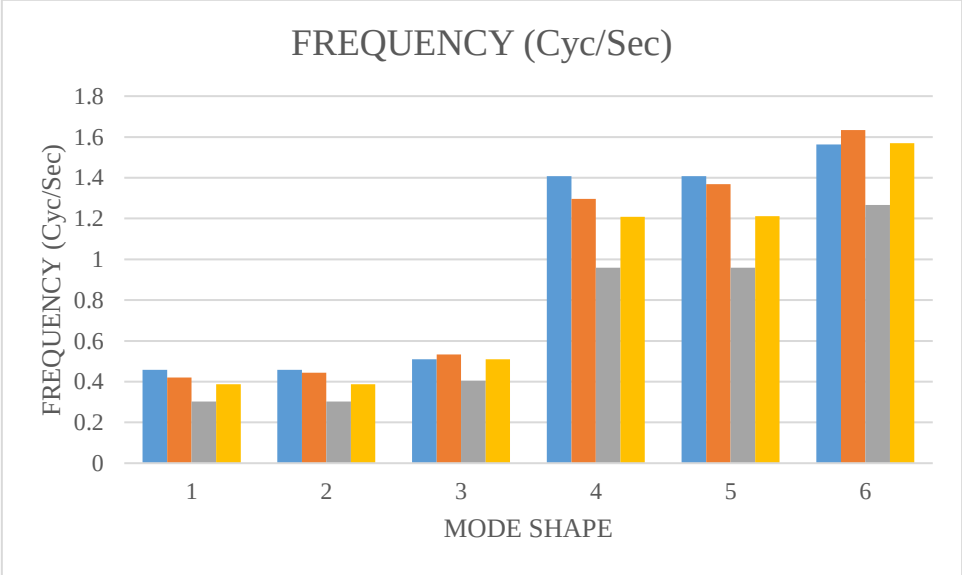

Graph 29: Frequency (Cyc/Sec)

The graph above illustrates the frequency (Cyc/Sec) results. The Y-axis represents frequency (Cyc/Sec), while the X-axis represents mode configurations.

With Mass Irregularity

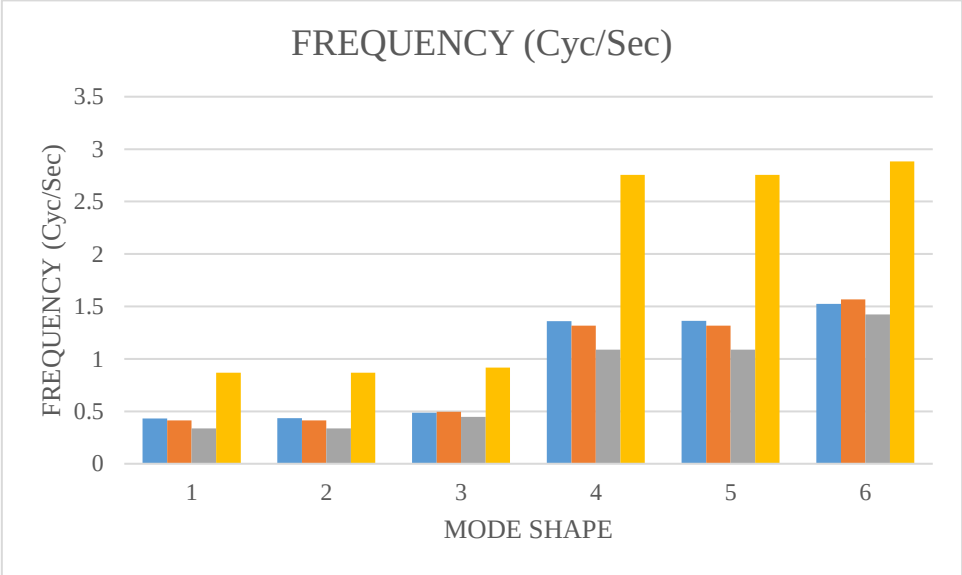

Graph 30: Frequency (Cyc/Sec)

Results for Frequency (Cyc/Sec) are displayed in the graph above. X indicates mode shapes, while Y indicates frequency (Cyc/Sec).

Conclusion:

A comprehensive examination was conducted in this research to contrast the mass irregularities observed in bubble deck slab systems and conventional slab systems in a range of structural configurations. Strict finite element analysis was conducted on the eight distinct models, consisting of irregular and non-irregular iterations of both systems, utilising the ETABS software. The analysis yielded valuable insights regarding the structural behaviour of the aforementioned systems, supplying details regarding their response to dynamic pressures.

The findings show that mass irregularities have a detectable effect on the behavior of high-rise buildings. When mass anomalies were present, maximum narrative displacement and tale drift increased, suggesting higher lateral movement under lateral stresses. However, bubble deck slab systems had more uniform distributions of base shear, responses, joint displacements, axial forces, bending moments, and shear forces. Because of this balanced load distribution, bubble deck slabs may provide improved structural integrity and resilience, especially in the face of seismic or dynamic events.

These results have substantial consequences for the building sector. They emphasize the need of taking unique project requirements into account while deciding between conventional as well as bubble deck slab systems. Factors such as the existence of mass irregularities, projected lateral loads, and overall structural performance goals should all be considered.

Finally, this research study is a helpful resource for engineers, architects, and stakeholders engaged in high-rise building development. The data-driven insights offered here may help you choose the best slab system for your project, improving structural performance, cost-effectiveness, and safety. As the construction industry evolves, this study emphasizes the need of continued research and real-world testing to evaluate and develop these results, assuring the best design and construction of high-rise buildings in the future.

Reference

[1] Abid, “Finite element simulation of vertical temperature gradients in a standard W40×235 steel beam,” *IOP Conf. Ser. Mater. Sci. Eng.*, vol. 988, no. 1, 2020, doi: 10.1088/1757-899X/988/1/012035.

[2] Al-Gasham, “Structural behavior of reinforced concrete one-way slabs voided by polystyrene balls,” *Case Stud. Constr. Mater.*, vol. 11, p. e00292, Dec. 2019, doi: 10.1016/J.CSCM.2019.E00292.

[3] T. Al-gasham, “Structural Performance of Reinforced Concrete Bubble Slabs after Exposing to Fire Flame Dr.,” no. April, 2017.

[4] T. S. Al-Gasham, J. M. Mhalhal, and H. A. Jabir, “Improving punching behavior of interior voided slab-column connections using steel sheets,” *Eng. Struct.*, vol. 199, p. 109614, Nov. 2019, doi: 10.1016/J.ENGSTRUCT.2019.109614.

[5] M. Amoushahi Khouzani, M. Zeynalian, M. Hashemi, D. Mostofinejad, and F. Farahbod, “Study on shear behavior and capacity of biaxial ellipsoidal voided slabs,” *Structures*, vol. 27, pp. 1075–1085, Oct. 2020, doi: 10.1016/J.ISTRUC.2020.07.017.

[6] J. H. Chung, H. K. Choi, S. C. Lee, and C. S. Choi, "Shear Capacity of Biaxial Hollow Slab with Donut Type Hollow Sphere," *Procedia Eng.*, vol. 14, pp. 2219–2222, Jan. 2011, doi: 10.1016/J.PROENG.2011.07.279.

[7] J. H. Chung, H. K. Choi, S. C. Lee, and C. S. Choi, "One-way shear strength of circular voided reinforced concrete floor slabs," *https://doi.org/10.1680/stbu.14.00044*, vol. 168, no. 5, pp. 336–350, Sep. 2015, doi: 10.1680/STBU.14.00044.

[8] J. H. Chung, H. S. Jung, B. il Bae, C. S. Choi, and H. K. Choi, "Two-Way Flexural Behavior of Donut-Type Voided Slabs," *Int. J. Concr. Struct. Mater.*, vol. 12, no. 1, pp. 1–13, Dec. 2018, doi: 10.1186/S40069-018-0247-6/FIGURES/13.

[9] J.-H. Chung, H.-K. Choi, S.-C. Lee, and C.-S. Choi, "Flexural Strength and Stiffness of Biaxial Hollow Slab with Donut Type Hollow Sphere," *J. Archit. Inst. Korea Struct. Constr.*, vol. 30, no. 5, pp. 3–11, May 2014, doi: 10.5659/JAIK_SC.2014.30.5.003.

[10] L. Chung, S. H. Lee, S. H. Cho, S. S. Woo, and K. K. Choi, "Investigations on Flexural Strength and Stiffness of Hollow Slabs," *http://dx.doi.org/10.1260/1369-4332.13.4.591*, vol. 13, no. 4, pp. 591–601, Nov. 2016, doi: 10.1260/1369-4332.13.4.591.

[11] Corey j midkiff B.S., "plastic voided slab systems: applications and design," pp. 1–4, 2013.

[12] R. Dewberry, "Two Dimensional Micromechanics Based Computational Model for Spherically Voided Biaxial Slabs (SVBS)," 2004.

[13] T. Gudmand-Høyer and Danmarks Tekniske Universitet. BYG. DTU, "Yield line theory for concrete slabs subjected to axial force : volume 2," 2003.

[14] A. M. Ibrahim, M. A. Ismael, and H. A. A. Hussein, "Effect of Construction Type on Structural Behaviour of R.C Bubbled One-Way Slab," *Diyala J. Eng. Sci.* , vol. 12, no. 1, pp. 73–79, Mar. 2019, doi: 10.24237/DJES.2019.12109.

[15] A. M. Ibrahim, M. A. Ismael, and H. A. S. Abdul Hussein, "the Effect of Balls Shapes and Spacing on Structural Behaviour of Reinforced Concrete Bubbled Slabs," *J. Eng. Sustain. Dev.*, vol. 23, no. 2, pp. 56–65, 2019, doi: 10.31272/jeasd.23.2.5.

[16] J. Jamal and J. Jolly, "A study on structural behaviour of bubble deck slab using spherical and elliptical balls," *Int. Res. J. Eng. Technol.*, pp. 2090–2095, 2017, [Online]. Available: www.irjet.net

[17] B. H. Kim, J. H. Chung, H. K. Choi, S. C. Lee, and C. S. Choi, "Flexural Capacities of One-Way Hollow Slab with Donut Type Hollow Sphere," *Key Eng. Mater.*, vol. 452–453, pp. 773–776, 2011, doi: 10.4028/WWW.SCIENTIFIC.NET/KEM.452-453.773.

[18] S. Kim, L. Cheng-gao, I. Kang, H. Lee, K. Lee, and K. Lee, "Punching Shear of I-Slab With Polystyrene Void Forms," pp. 14–17, 2008.

[19] T. Lai and D. Veneziano, "Structural behavior of BubbleDeck® slabs and their application to lightweight bridge decks," 2010. [Online]. Available: https://dspace.mit.edu/handle/1721.1/60774

[20] C. H. Lee, I. Mansouri, E. Kim, J. Ryu, and W. T. Woo, "Experimental analysis of one-way composite steel deck slabs voided by circular paper tubes: Shear strength and moment–shear interaction," *Eng. Struct.*, vol. 182, pp. 227–240, Mar. 2019, doi: 10.1016/J.ENGSTRUCT.2018.12.063.

[21] Maciej Serda *et al.*, "Structural Behaviour of Bubble Deck Slabs and its Application," *Int. J. Sci. Res. Dev.*, vol. 4, no. 2, pp. 433–437, May 2016, doi: 10.2/JQUERY.MIN.JS.

[22] C. J. Midkiff and K. W. Kramer, "plastic voided slab systems: applications and design," 2013.

[23] H. T. Nimnim and Z. M. J. Z. Alabdeen, "structural behavior of voided normal and high strength reinforced concrete slabs," vol. 10, no. 2, pp. 1–11, 2019.

[24] R. Nuraeni *et al.*, "Bubble Deck," *Diponegoro J. Account.*, vol. 2, no. 1, pp. 2–6, 2017, [Online]. Available: http://i-lib.ugm.ac.id/jurnal/download.php?dataId=2227%0A???%0Ahttps://ejournal.unisba.ac.id/index.php/kajian_akuntansi/article/view/3307%0Ahttp://publicacoes.cardiol.br/portal/ijcs/portugues/2018/v3103/pdf/3103009.pdf%0Ahttp://www.scielo.org.co/scielo.ph

[25] R. Sagadevan and B. N. Rao, "Effect of void former shapes on one-way flexural behaviour of biaxial hollow slabs," *Int. J. Adv. Struct. Eng.*, vol. 11, no. 3, pp. 297–307, Sep. 2019, doi: 10.1007/S40091-019-0231-7/FIGURES/17.

[26] R. Sagadevan and B. N. Rao, "Experimental and analytical investigation of punching shear capacity of biaxial voided slabs," *Structures*, vol. 20, pp. 340–352, Aug. 2019, doi: 10.1016/J.ISTRUC.2019.03.013.

[27] M. Schnellenbach-Held and K. Pfeffer, "Punching behavior of biaxial hollow slabs," *Cem. Concr. Compos.*, vol. 24, no. 6, pp. 551–556, Dec. 2002, doi: 10.1016/S0958-9465(01)00071-3.

[28] A. Shetkar, "an experimental study on bubble deck slab system with elliptical balls," 2015.